Supporting Information

Rationally engineered smart automotive upholstery leather based on gradient feeding *in situ* one-pot reaction in microreactors of natural skin

Qingxin Han,[a, b, #, *] Huishu Fan,[a, #] Xuechuan Wang,[b] Junli Zhang,[a] Xinhua Liu,[b] and Xiaoyu Guan[b, *]

[a] College of Bioresources Chemistry and Materials Engineering, Shaanxi University of Science and Technology, Xi'an, 710021, China.

[b] Institute of Biomass & Functional Materials, Shaanxi University of Science & Technology, Xi'an, 710021, China.

[*] Corresponding author: hanqingxin@sust.cn; guanxiaoyu@sust.edu.cn.

[#] These authors contributed to the work equally and should be regarded as co-first authors.

Table of Contents

1. Preparation:

1.1. Preparation of ATP-KH560

ATP (6 g) and sodium hexametaphosphate (0.18 g) were dissolved in 300 mL of deionized water and stirred at 50 °C for 1 hour. The resulting mixture was then centrifuged at 2000 rpm for 10 minutes to obtain the supernatant, a dispersion of ATP rod crystals. A mixture of KH560 and the ATP dispersion was prepared at a mass ratio of 2:3 (KH560 to ATP) and stirred at 300 rpm for 1.5 hours at 50 °C, resulting in the formation of ATP-KH560.

1.2. Preparation of CS-GTE

For the preparation of CS-GTE, chitosan (1.3638 g) was first dissolved in 50 mL of deionized water, followed by the addition of triethylamine (0.08 g) and GTE (1.65 g). The mixture was then stirred for 2 hours at 40 °C with a stirring rate of 300 rpm to obtain the CS-GTE complex.

2. Supporting Figures:

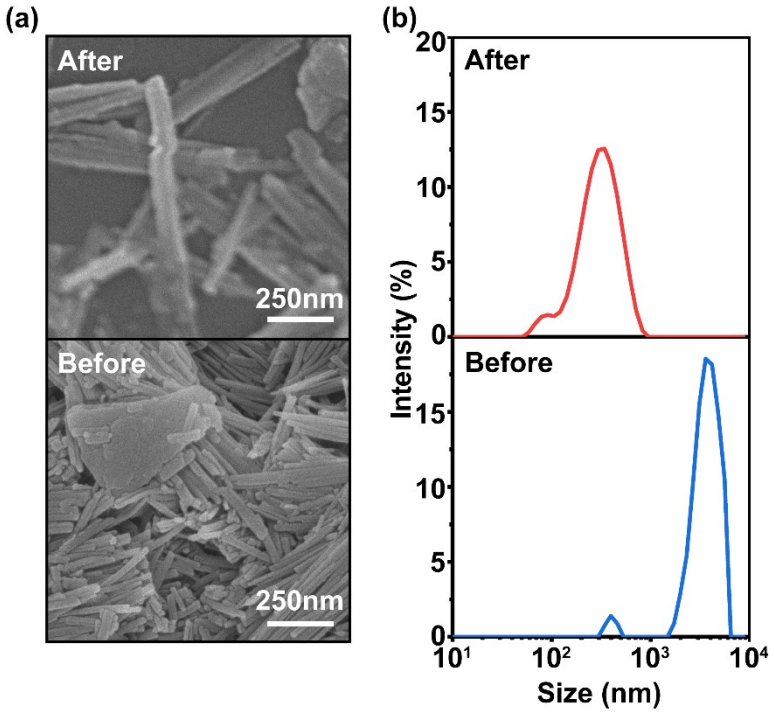

Figure S1. SEM images (a) and particle size distribution graph (b) before and after ATP dispersion.

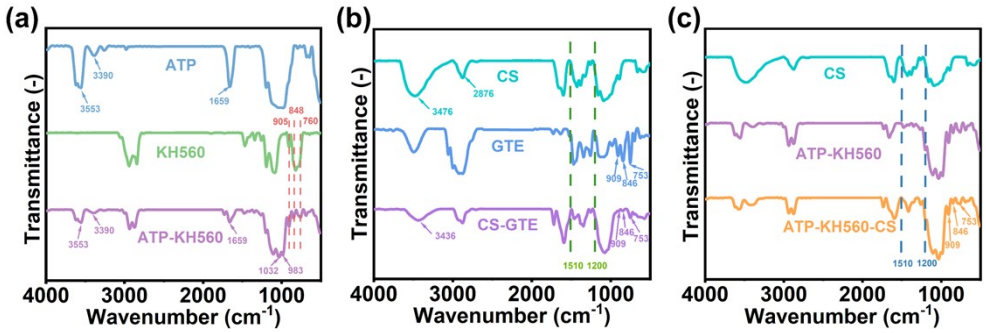

Figure S2. FTIR spectrum images for ATP, KH560, ATP-KH560, CS, GTE, CS-GTE, and ATP-KH560-CS.

As shown in Fig. S2a, the bands at 3553 cm^{-1} and 3390 cm^{-1} are attributed to the stretching vibrations of Al-OH and Fe-OH on ATP; the band at 1659 cm^{-1} is attributed to the -OH stretching vibration in ATP.[1] Characteristic absorption peaks were shown at 909, 846, and 753 cm^{-1}, which can be attributed to the terminal epoxy group in KH560. Meanwhile, the decrease in peak areas at 3553 cm^{-1}, 3390 cm^{-1}, and 1659 cm^{-1} and the appearance of additional peaks at 1032 cm^{-1}, and 983 cm^{-1} are attributed to the reaction of ATP with KH560 to form the S-oxide group. KH560 reaction to the stretching vibration of the Si-O-Si bond.[2] In particular, the prepared ATP-KH560 after the interaction of ATP with KH560 showed absorption peaks at 909, 846, and 753 cm^{-1}, which are typical characteristic peaks of terminal epoxy groups. As shown in Fig. S2b, the band at 3476 cm^{-1} can be attributed to the stretching vibrations of O-H and N-H in the methylene groups of CS.[3] The characteristic bands at 909, 848, and 755 cm^{-1} can be attributed to the terminal epoxy groups in GTE.[4] After the interaction of CS and GTE, the resultant CS-GTE molecule, as compared to CS, the 3436 cm^{-1} where the characteristic peaks at, were red-shifted. This may be due to the reaction of GTE with the free amino and primary alcohol hydroxyl groups of CS. The decrease in the peak area of CS-GTE in the 1510-1200 cm^{-1} band compared with both CS and GTE may be due to

the reaction of the amino group of CS with the epoxy group of GTE, which introduces the -CH_2 group. In particular, after the interaction of CS with GTE, the prepared CS-GTE showed characteristic absorption peaks at 909, 846, and 753 cm^{-1}, which are typical of terminal epoxy groups,[4] suggesting that GTE was successfully grafted onto CS to generate products containing terminal epoxy groups. Meanwhile, in this work, a simulation experiment was done in vitro in leather by adding CS to ATP-KH560 for the reaction, and as shown in Fig. S2c, the peak area of ATP-KH560-CS increased in the 1510-1200 cm^{-1} band compared to CS, which was attributed to the epoxy group in ATP-KH560 reacting with the amino group of CS and introducing the -CH_2 group. In addition, the characteristic bands of ATP-KH560-CS at 909, 848, and 755 cm^{-1} confirm the presence of epoxy groups in the material. All these phenomena verified that CS could react with ATP-KH560 inside the leather, which subsequently indicated that CS-GTE could enhance the cross-linking between ATP-KH560 and leather collagen. It is GTE that reacts with the amino group and the hydroxyl group of the primary alcohol in CS.

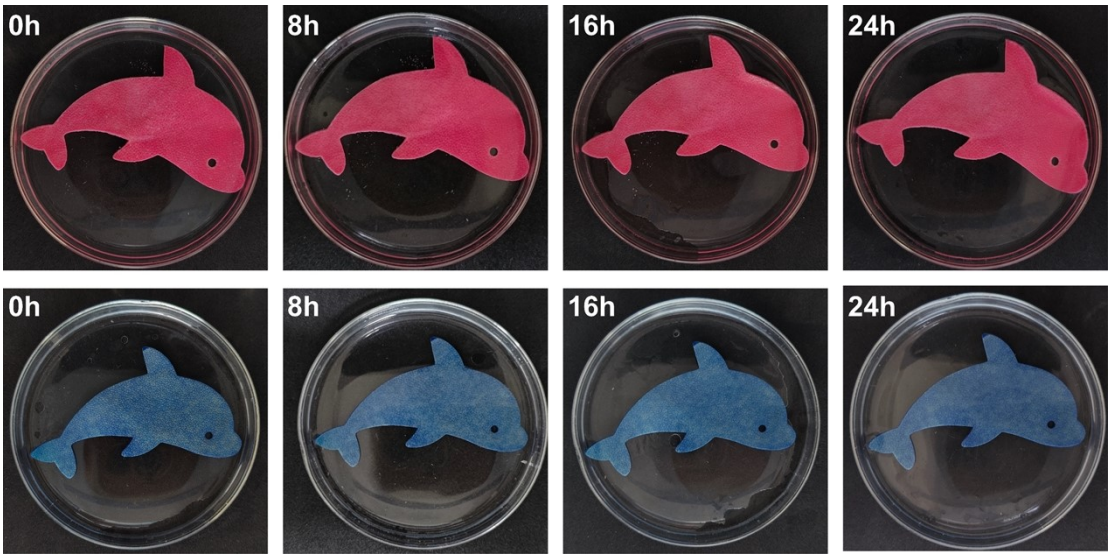

Figure S3 Digital photographs of ACG leather samples dyed with normal and fluorescent dyes and immersed in water for 0, 8, 16 and 24 hours respectively.

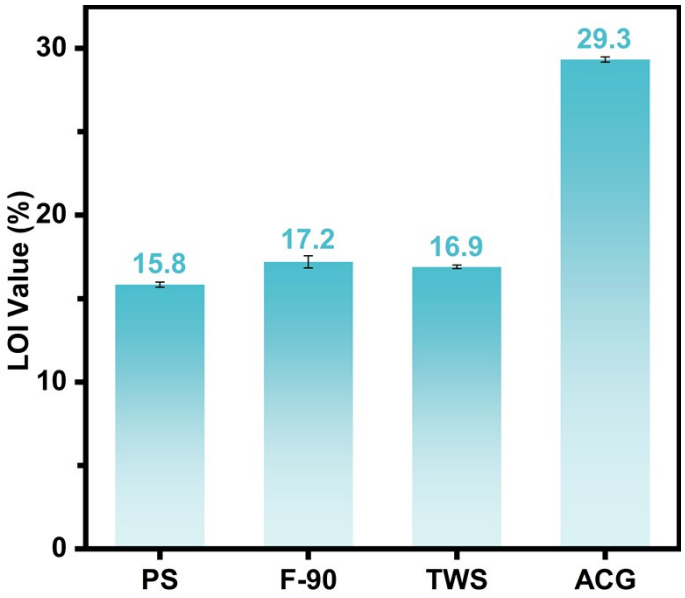

Figure S4. LOI values of different samples.

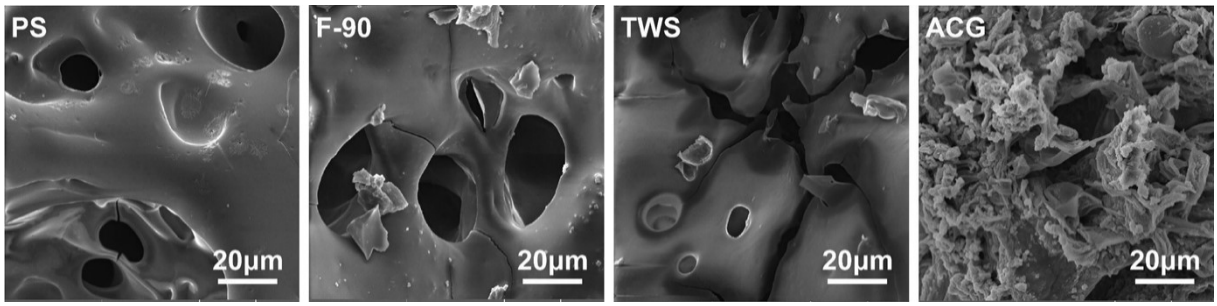

Figure S5. The electron micrographs of the cross-section of its post-combustion residual samples.

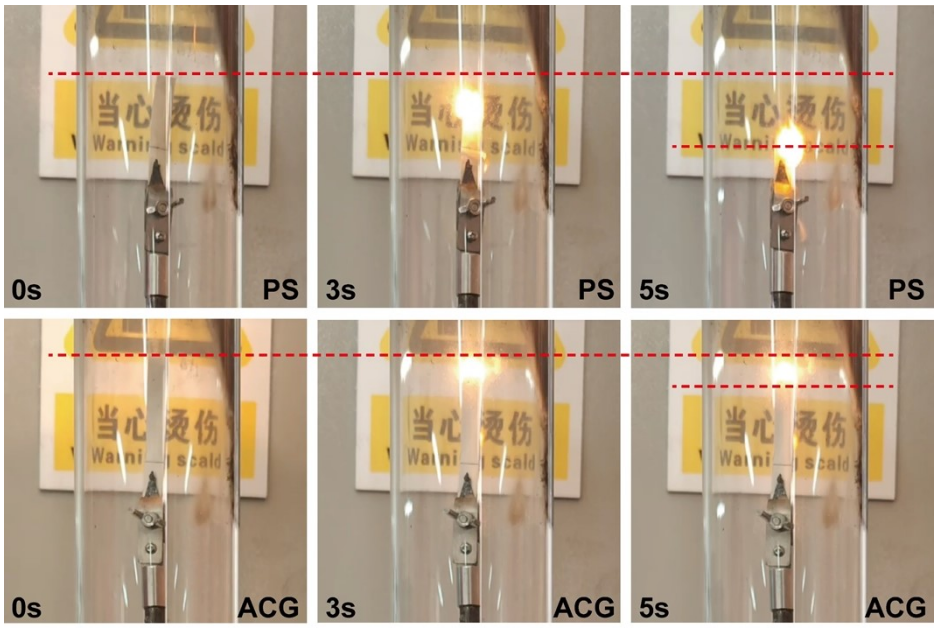

Figure S6. Digital images of PS and this work at 0s, 3s, and 5s in an environment with an LOI value (%) of 30%.

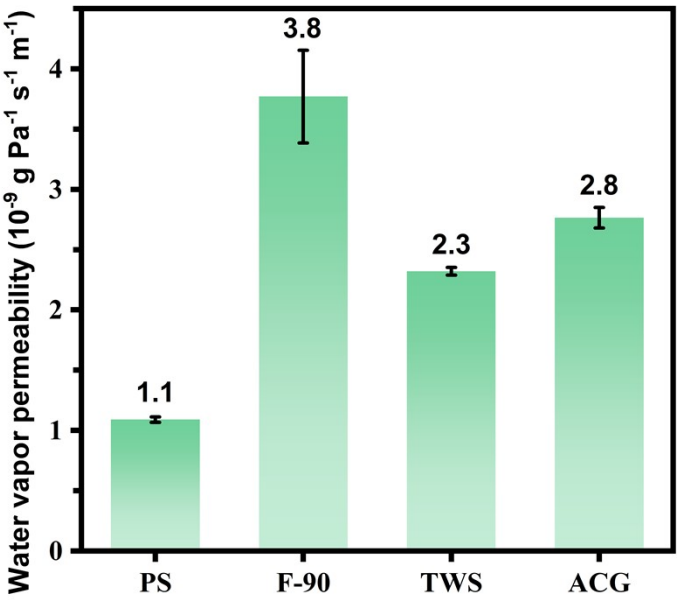

Figure S7. Water vapor permeability of different samples.

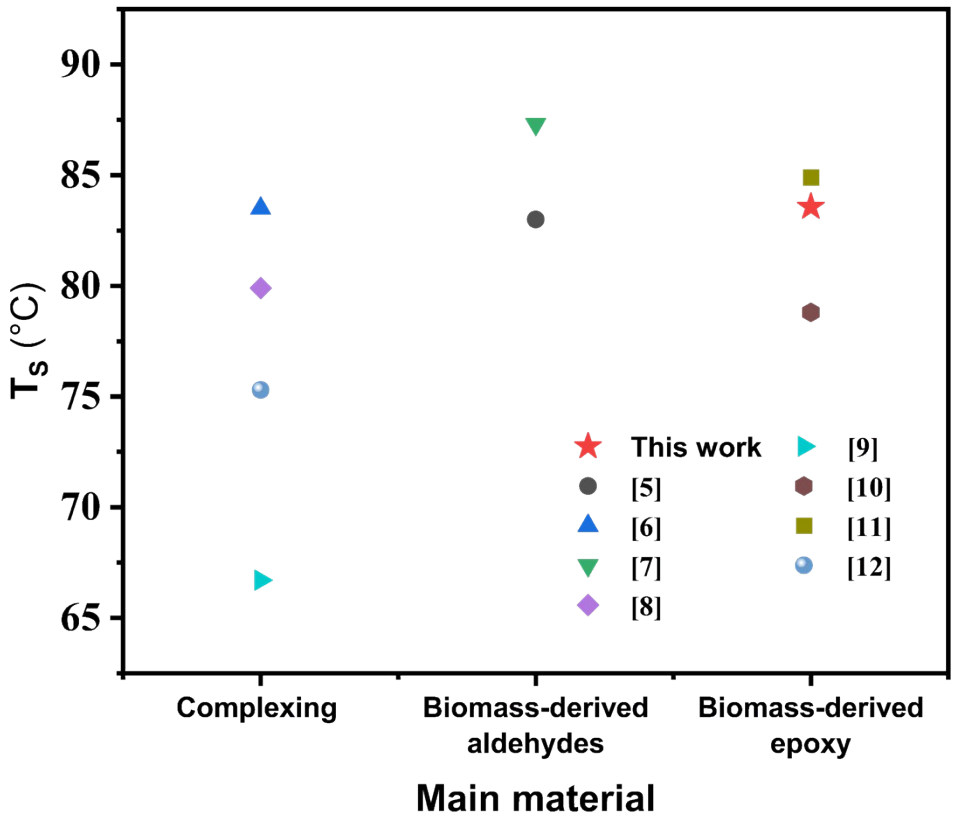

Figure S8. Comparison of shrinkage temperatures for traditional leathers prepared from biomass epoxy, biomass-deried aldehydes, and complexing.

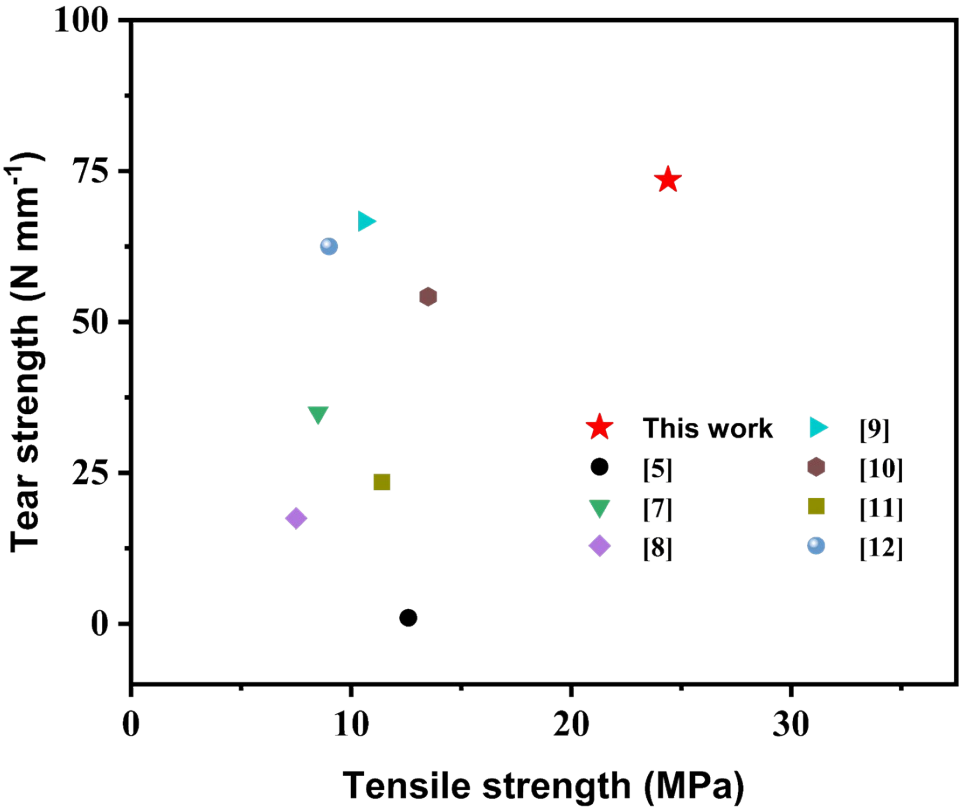

Figure S9. Comparison of tensile strength and tear strength for traditional leathers prepared from biomass epoxy, biomass-deried aldehydes, and complexing.

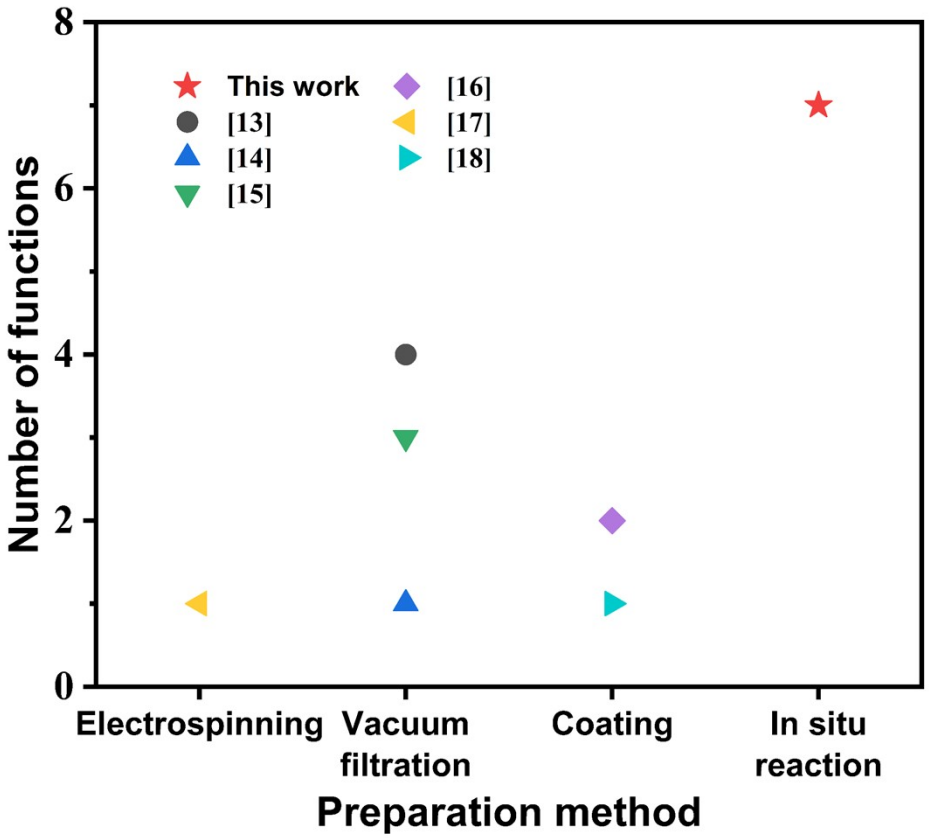

Figure S10. Comparison of the number of functions exhibited by single-functional and multifunctional leather-based materials, as well as leather-like materials, produced through different preparation processes.

3. Supporting tables:

Table S1. Tanning processes of TWS tanning agents.

Operation	material	Dosage [a)] [%]	Temperature [℃]	Time [min]	Remarks
Washing	Water	150	25	20	Check pH,until the pH is 7±,continue the mechanical action for 20 min and drain.
	Salt	7			
	$NaHCO_3$	0.6			
Tanning	Water	150	25	180	Check pH,until the pH is 7±,continue the mechanical action for 180 min.
	$NaHCO_3$/ Na_2CO_3	0.5			
	TWS	10			
Basification	$NaHCO_3$/ Na_2CO_3	0.6	40	240	Check pH,until the

					pH is 7±,continue the mechanical action for 240 min, then stay overnight..

[a)]The dosages of materials are based on 1.5 times the weight of PS.

Table S2. Tanning processes of F-90 tanning agents.

Operation	**material**	**Dosage[a)] [%]**	**Temperature [℃]**	**Time [min]**	**Remarks**
Washing	Water	150	25	20	Check pH,until the pH is 7±,continue the mechanical action for 20 min and drain.
	Salt	7			
	$NaHCO_3$	0.6			
Tanning	F-90	10	37	120	Check pH,until the

	Water	40			pH is 7±,continue the mechanical action for 120 min.
	$NaHCO_3$/ Na_2CO_3	0.6			
	Water	40			Check pH,until the pH is 6.5±,continue the mechanical action for 120 min.
	CH_2O_2	0.6	40	120	
	Water	40			Check pH,until the pH is 4.5±,continue the mechanical action for 120 min.
	CH_2O_2	0.6	45	120	
Washing	Water	150	40	20	continue the mechanical

	action for 20 min then drain..

[a)]The dosages of materials are based on 1.5 times the weight of PS.

Table S3. Comparison of the number of functions exhibited by single-functional and multifunctional leather-based materials, as well as leather-like materials, produced through different preparation processes.

	Preparation method	Functions									Ref.
		Thermal management	EMI shielding effectiveness	Noise reduction	Color modulation	Bactericidal	Flame retardancy	As an electrode	Sensing	Soil degradation	
This work	In situ reaction	+	+	+	+	+	+	-	-	+	-
Leather-based functional materials	Vacuum filtration	+	+	-	-	-	-	+	+	-	[13]
	Vacuum filtration	+	+	-	-	-	-	-	+	-	[14]
	Vacuum filtration	+	+	-	-	-	-	-	+	-	[15]
	Coating	+	+	-	-	-	-	-	-	-	[16]
Leather-like functional materials	Electrospinning	+	-	-	-	-	-	-	-	-	[17]
	Coating	-	+	-	-	-	-	-	-	-	[18]

References:

[1] F. Duan, Y. Zhu, H. Zhang, Y. Lu, A. Wang. Effect of structural evolution of attapulgite on pickering foam and fabrication of porous materials for removal methylene blue. *Chem. Eng. J.* 2023, **474**, 145942.

[2] Z. Shen, W. Gao, P. Li, X. Wang, Q. Zheng, H. Wu, Y. Ma, W. Guan, S. Wu, Y. Yu, K. Ding. Highly sensitive nonenzymatic glucose sensor based on nickel nanoparticle‐attapulgite-reduced graphene oxide-modified glassy carbon electrode. *Talanta* 2016, **159**, 194.

[3] S. Feng, S. Dai, Z. Wei, J. Wang, N. Xiang, P. Shao. Soy conglycinin amyloid fibril and chitosan complex scaffold for cultivated meat application. *Food Hydrocolloid.* 2024, **153**, 110017.

[4] Z. Dai, L. Ansaloni, D. L. Gin, R. D. Noble, L. Deng. Facile fabrication of co2 separation membranes by cross-linking of poly(ethylene glycol) diglycidyl ether with a diamine and a polyamine-based ionic liquid. *J. Membr. Sci.* 2017, **523**, 551.

[5] W. Ding, X. Pang, Z. Ding, D. C. W. Tsang, Z. Jiang, B. Shi. Constructing a robust chrome-free leather tanned by biomass-derived polyaldehyde via crosslinking with chitosan derivatives. *J. Hazard. Mater.* 2020, **396**, 122771.

[6] Z. Jiang, M. Gao, W. Ding, C. Huang, C. Hu, B. Shi, D. C. W. Tsang. Selective degradation and oxidation of hemicellulose in corncob to oligosaccharides: from biomass into masking agent for sustainable leather tanning. *J. Hazard. Mater.* 2021, **413**, 125425.

[7] W. Ding, Y. Yi, Y. Wang, J. Zhou, B. Shi. Peroxide-periodate co-modification of carboxymethylcellulose to prepare polysaccharide-based tanning agent with high solid content. *Carbohydr. Polym.* 2019, **224**, 115169.

[8] J. Chen, J. Ma, Q. Fan, W. Zhang, R. Guo. A sustainable chrome-free tanning approach based on zr-mofs functionalized with different metals through post-synthetic modification.

Chem. Eng. J. 2023, **474**, 145453.

[9] Y. Shen, J. Ma, Q. Fan, D. Gao, H. Yao. Strategical development of chrome-free tanning agent by integrating layered double hydroxide with starch derivatives. *Carbohydr. Polym.* 2023, **304**, 120511.

[10] D. Hao, X. Wang, O. Yue, S. Liang, Z. Bai, J. Yang, X. Liu, X. Dang. A "wrench-like" green amphoteric organic chrome-free tanning agent provides long-term and effective antibacterial protection for leather. *J. Cleaner Prod.* 2023, **404**, 136917.

[11] D. Hao, X. Wang, S. Liang, O. Yue, X. Liu, D. Hao, X. Dang. Sustainable leather making — an amphoteric organic chrome-free tanning agents based on recycling waste leather. *Sci. Total Environ.* 2023, **867**, 161531.

[12] J. Chen, J. Ma, Q. Fan, W. Zhang. An eco-friendly metal-less tanning process, zr-based metal-organic frameworks as novel chrome-free tanning agent. *J. Cleaner Prod.* 2023, **382**, 135263.

[13] Q. Guo, J. Guo, H. Chen, P. Zhou, C. Li, K. Yang, N. Hua, J. Wang, M. Weng. Multi-functional graphene/leather for versatile wearable electronics. *J. Mater. Chem. A* 2023, **11**, 11773-11785.

[14] Z. Ma, X. Xiang, L. Shao, Y. Zhang, J. Gu. Multifunctional wearable silver nanowire decorated leather nanocomposites for joule heating, electromagnetic interference shielding and piezoresistive sensing. *Angew. Chem. Int. Ed.* 2022, **61**, e202200705.

[15] Z. Fan, L. Lu, M. Sang, J. Wu, X. Wang, F. Xu, X. Gong, T. Luo, K. C. Leung, S. Xuan. Wearable safeguarding leather composite with excellent sensing, thermal management, and electromagnetic interference shielding. *Adv. Sci.* 2023, **10**, e2302412.

[16] C. Mo, X. Lei, X. Tang, M. Wang, E. Kang, L. Xu, K. Zhang. Nanoengineering natural leather for dynamic thermal management and electromagnetic interference shielding. *Small* 2023, **19**, e2303368.

[17] N. Cheng, Z. Wang, Y. Lin, X. Li, Y. Zhang, C. Ding, C. Wang, J. Tan, F. Sun, X. Wang, J. Yu, B. Ding. Breathable dual-mode leather-like nanotextile for efficient daytime radiative cooling and heating. *Adv. Mater.* 2024, **36**, e2403223.

[18] J. Li, M. Cui, J. Wen, Y. Chen, B. Shi, H. Fan, J. Xiang. Leather-like hierarchical porous composites with outstanding electromagnetic interference shielding effectiveness and durability. *Composites Part B* 2021, **225**, 109272.